Developmental and Comparative Immunology 47 (2014) 104–114

Contents lists available at ScienceDirect

Developmental and Comparative Immunology

journal homepage: www.elsevier.com/locate/dci

# Molecular profile and functional characterization of the ferritin H subunit from rock bream (*Oplegnathus fasciatus*), revealing its putative role in host antioxidant and immune defense

Don Anushka Sandaruwan Elvitigala [a,b], Thanthrige Thiunuwan Priyathilaka [a,b], Bong-Soo Lim [b], Ilson Whang [a,b], Sang-Yeob Yeo [c], Cheol Young Choi [d], Jehee Lee [a,b,*]

[a] Department of Marine Life Sciences, School of Marine Biomedical Sciences, Jeju National University, Jeju Self-Governing Province 690-756, Republic of Korea
[b] Fish Vaccine Research Center, Jeju National University, Jeju Special Self-Governing Province 690-756, Republic of Korea
[c] Department of Biotechnology, Division of Applied Chemistry & Biotechnology, Hanbat National University, Daejeon 305-719, Republic of Korea
[d] Division of Marine Environment and Bioscience, Korea Maritime University, Busan 606-791, Republic of Korea

ARTICLE INFO

*Article history:*
Received 3 April 2014
Revised 1 July 2014
Accepted 3 July 2014
Available online 11 July 2014

*Keywords:*
Ferritin H
Rock bream
Recombinant protein
Functional analysis
Pathogen-induced expressional regulation

ABSTRACT

Ferritins are iron binding proteins made out of 24 subunits, involved in iron homeostasis and metabolism in cellular environments. Here, we sought to identify and functionally characterize a one type of subunits of ferritin (ferritin H-like subunit) from rock bream (*Oplegnathus fasciatus*; RbFerH). The complete coding sequence of *RbFerH* was 531 bp in length, encoding a 177-amino acid protein with a predicted molecular mass of 20.8 kDa. The deduced protein structure possessed the domain architecture characteristic of known ferritin H subunits, including metal ligands for iron binding, a ferroxidase center, and two iron-binding region signatures. As expected, the 5′ untranslated region of the *RbFerH* cDNA sequence contained a putative iron response element region, a characteristic regulatory element involved in its translation. The *RbFerH* gene comprised 5 exons and 4 introns spanning a 4195 bp region. Overexpressed recombinant RbFerH protein demonstrated prominent Fe(II) ion depriving activity, bacteriostatic properties, and protective effects against oxidative double-stranded DNA damage. Using quantitative polymerase chain reaction (qPCR), we found that *RbFerH* was expressed ubiquitously in the majority of physiologically important tissues in rock bream. A greater abundance of the mRNA transcripts were detected in blood and liver tissues. Upon administering different microbial pathogens and pathogen-derived mitogens, *RbFerH* transcription was markedly elevated in the blood of rock bream. Taken together, our findings suggest that RbFerH acts as a potent iron sequestrator in rock bream and may actively participate in antimicrobial as well as antioxidative defense.



## 1. Introduction

Iron, a vital element found abundantly in living organisms has indispensable roles in an array of biological events including metabolic redox processes. However, excessive levels of reduced or free iron in cells can lead to detrimental toxic effects. Fenton-type reactions involving in the catalysis of free Fe(II) ions in cellular environments induces reactive oxygen species (ROS)-mediated oxidative stress (Crichton et al., 2002). Therefore, proper *in vivo* regulation of free iron availability is required for the survival of living cells. This is facilitated by balancing the uptake of iron through increasing the efficacy of iron transport and storage. Ferritins play a major role in iron storage by binding excessive free Fe(II) ions in cellular environments, releasing them only in times of iron shortage (Watt, 2011). Thus, ferritin is involved in iron detoxification through its iron binding property, maintaining iron homeostasis and limiting iron bioavailability to nontoxic levels.

Ferritins are ubiquitously distributed proteins in both prokaryotes and eukaryotes. Three-dimensionally, eukaryotic ferritin is arranged into a hollow spherical protein complex consisting of 24 subunits that can mineralize approximately 4500 iron atoms inside its thick protein shell (Crichton and Declercq, 2010). In the vertebrate lineage, two ferritin subunits encoded by distinct genes have been identified (Caskey et al., 1983; Worwood et al., 1985).

* Corresponding author at: Marine Molecular Genetics Lab, Department of Marine Life Sciences, College of Ocean Science, Jeju National University, 66 Jejudaehakno, Ara-Dong, Jeju, 690-756, Republic of Korea. Tel.: +82 64 754 3472; fax: +82 64 756 3493.
*E-mail address:* jehee@jejunu.ac.kr (J. Lee).

http://dx.doi.org/10.1016/j.dci.2014.07.004
0145-305X/

Heavy (H) and light (L) chain ferritin subunits (Arosio et al., 2009) have molecular masses ranging between 18 and 28 kDa. Ferritin H subunits are characterized by their unique ferroxidase center involved in Fe(II) ion binding (Lawson et al., 1991). The L subunits, on the other hand, are identified by their iron nucleation sites that allow ligands to bind Fe(III) ions. The ferritin ferroxidase center recognizes and binds Fe(II) ions that become oxidized to Fe(III) ions by dioxygen (Lawson et al., 1989). Fe(III) then binds to nucleation sites to undergo the mineralization process (Santambrogio et al., 1996). The composition ratio of H and L subunits in ferritin can vary greatly depending on the tissue type and physiological status of different cells. For instance, H-rich ferritins are abundant in heart and kidney tissues, whereas L-rich ferritins are more abundant in the liver and spleen (Arosio et al., 1976). In addition to the two main ferritin subunits, a third middle (M) subunit has been identified., The M subunit shows characteristic features and functions of both H and L subunits which is commonly found in fish and amphibians (Andersen et al., 1995; Dickey et al., 1987; Zheng et al., 2010a).

Ferritins have been identified in a diverse group of living organisms including microorganisms, plants, and most vertebrate and invertebrate species, examined. The ferritins from different species share common features (Theil, 1987). Ferritins are predominantly cytosolic proteins; however, they are also present in the mitochondria in some insects (Missirlis et al., 2006) and both mitochondria and nuclei of several mammalian cell types, protecting these organelles from iron toxicity and oxidative damage. Ferritins are also found in the plastids of plant cells and secreted forms have been identified in insects (Andrews et al., 1992; Arosio et al., 2009). Further, regarding their function in iron metabolism, ferritins reportedly play a significant role in other biological processes including cell activation, development, immune defense, and angiogenesis (Alkhateeb and Connor, 2010; Coffman et al., 2008; Parthasarathy et al., 2002; Wang et al., 2010). Expression of the ferritin subunits is tightly regulated at the transcriptional and post-transcriptional levels. Iron responsive element binding proteins have a major role in their transcriptional regulation (Outten and Theil, 2009; Theil, 2007; Torti and Torti, 2002). These regulatory mechanisms cooperatively control the amount of ferritin that is expressed in or secreted from cells. Exogenous conditions such as pathogen infection (Zheng et al., 2010a), xenobiotic stress (Torti and Torti, 2002), iron load (Wu et al., 2010), temperature stress (Salinas-Clarot et al., 2011), pH stress (Zhou et al., 2008), and endogenous factors like oxidative stress (Zheng et al., 2010a), and inflammatory cytokines (Torti and Torti, 2002) also regulate the expression of ferritin subunit genes at the transcriptional level.

As previously reported, both ferritin H and M subunits were already identified from Atlantic salmon (*Salmo salar*), from which H subunit was found to express mainly in spleen, liver and heart, whereas M chain was exclusively expressed in gonads (Andersen et al., 1995). Interestingly, three isoforms of ferritin H subunits were identified form rainbow trout (*Oncorhynchus mykiss*) and detected their cold inducible gene expression (Yamashita et al., 1996). Recent reports on teleostan ferritin M and H subunits suggests that teleostan ferritins may involve in host immune responses besides its main role in iron homeostasis, further participating in host antioxidant defense (Elvitigala et al., 2013; Liu et al., 2010; Zhang et al., 2010; Zheng et al., 2010a,b). However, detailed characterizations and functional analyses of ferritin H orthologs have been performed in a limited number of teleost species including catfish (*Ictalurus punctatus*) (Liu et al., 2010), turbot (*Scophthalmus maximus*) (Zheng et al., 2010b), sea bass (*Dicentrarchus labrax*) (Neves et al., 2009), and the Atlantic salmon (*S. salar*) (Andersen et al., 1995). Therefore, our knowledge regarding teleost ferritin H orthologs is incomplete.

Mariculture farming has become an indispensable source of foods enriched in essential amino and fatty acids. Rock bream (*Oplegnathus fasciatus*), an edible maricultured fish species, is an important aqua-crop. It accounts for a considerable fraction of the total annual fish yield, making rock bream a profitable species in the global aqua-farming industry, particularly in East and South East Asia. However, considerable production loss of this maricultured species has been incurred recently, primarily because of the prevalence of bacterial and viral infections (Do et al., 2004; Mohanty and Sahoo, 2007) Thus, development of novel disease management strategies is essential to improve rock bream aqua-farming yields. Investigation into the naturally existing host immune defense mechanisms and strategies may contribute substantially towards this effort.

In this study, we identified and molecularly characterized a ferritin H-like subunit from rock bream (RbFerH), and investigated its functional role in iron(II) deprivation, antibacterial defense, and antioxidative defense by using recombinant RbFerH protein (rRbFerH). The tissue-specific expression of *RbFerH* was analyzed in several physiologically important tissues. In addition, we examined the regulation of *RbFerH* transcription in response to bacterial and viral fish pathogens along with their mitogens.

## 2. Materials and methods

### 2.1. Identification and sequence analysis of RbFerH

To identify the full-length cDNA sequence of *RbFerH*, we analyzed rock bream DNA sequence data from a cDNA library constructed previously (Whang et al., 2011a), using the Basic Local Alignment Search Tool (BLAST) algorithm (http://blast.ncbi.nlm.nih.gov/Blast.cgi). The identified *RbFerH* sequence was characterized using several *in silico* tools. The putative complete open reading frame (ORF) of *RbFerH* was identified and the corresponding amino acid sequence was deduced using the DNAsist 2.2 software. Protein domains were predicted using the ExPASy Prosite database (http://prosite.expasy.org). Physicochemical properties were determined using the ExPASy ProtParam tool (http://web.expasy.org/protparam). Pairwise and multiple sequence comparisons of RbFerH with its homologues were performed using the EMBOSS needle (http://Ebi.ac.uk/Tools/emboss/align) and ClustalW2 (http://Ebi.ac.uk/Tools/clustalw2) programs, respectively. The phylogenetic reconstruction of RbFerH and its orthologs was generated by the neighbor-joining method using Molecular Evolutionary Genetics Analysis version 4.0 (MEGA 4.0) software (Tamura et al., 2007).

The complete gene sequence of *RbFerH* was also identified in a custom constructed rock bream random-shear bacterial artificial chromosome (BAC) genomic DNA library (Lucigen®, USA). The BAC clone bearing the *RbFerH* gene was identified using a two-step polymerase chain reaction (PCR)-based genomic library screening approach using gene specific-primers (RbFerHqF and RbFerHqR; Table 1). The putative *RbFerH*-containing clone was then sequenced using the GS-FLX™ system (Macrogen, Korea) to obtain full-length genomic sequence. Using the National Center for Biotechnology Information (NCBI) Spidey online server (http://www.ncbi.nlm.nih.gov/spidey) and previously identified full-length *RbFerH* cDNA sequences, we annotated the exon–intron arrangement. Annotated sequence information for *RbFerH* was deposited in the NCBI GenBank database (accession number KJ461740).

### 2.2. Expression and purification of recombinant RbFerH fusion protein

rRbFerH fused to maltose binding protein (MBP) was expressed and purified as previously described, but with some modifications (Umasuthan et al., 2011). Briefly, the coding sequence of the *RbFerH* gene was amplified using the sequence-specific primers

**Table 1**
Oligomers used in this study.

| Name | Purpose | Sequence (5′ → 3′) |
|---|---|---|
| RbFerH-qF | BAC library screening and qPCR of *RbFerH* | GGATGACCAGGCATTGCACAACTT |
| RbFerH-qR | BAC library screening and qPCR of *RbFerH* | AGGGACTGGTTCACGCTCTTCT |
| RbFerH-F | ORF amplification (*Eco*RI) | GAGAGAgaattcATGAGTTCCCAGGTGAGACAGAACTTCC |
| RbFerH-R | ORF amplification (*Hin*dIII) | GAGAGAaagcttTTAGCTGCTTTCTTTGCCCAGGGT |
| Rb-βF | qPCR for rock bream β-actin gene | TCATCACCATCGGCAATGAGAGGT |
| Rb-βR | qPCR for rock bream β-actin gene | TGATGCTGTTGTAGGTGGTCTCGT |

RbFerH-F and RbFerH-R, which contained restriction enzyme sites for *Eco*RI and *Hin*dIII, respectively (Table 1). PCR was performed in a TaKaRa thermal cycler (TaKaRa, Japan) in a total volume of 50 μL containing 5 U TaKaRa ExTaq polymerase, 5 μL of 10× TaKaRa ExTaq buffer, 8 μL 2.5 mM dNTPs, 80 ng of template, and 20 pmol of each primer. The PCR was performed under the following conditions: initial denaturation at 94 °C for 3 min, followed by 35 cycles of 94 °C for 30 s, 57 °C for 30 s, 72 °C for 1 min, with a final extension at 72 °C for 5 min. The PCR product (~534 bp) was resolved on a 1% agarose gel, excised, and purified using the Expin™ Gel SV kit (GeneAll., Korea). Digested pMAL-c2X vector (170 ng) and PCR product (40 ng) were ligated using Mighty Mix (5.0 μl; TaKaRa) at 4 °C overnight. The ligated pMAL-c2X/RbFerH product was transformed into DH5α cells and sequenced. After sequence validation, the recombinant expression plasmid was transformed into *Escherichia coli* BL21 (DE3) competent cells. Expression of the rRbFerH fusion protein was induced using isopropyl-β-D-galactopyranoside (IPTG, 1 mM). *E. coli* cells were grown in 500 mL Luria broth (LB) supplemented with ampicillin (100 μg/mL) and glucose (0.2%) at 37 °C for 3 h. Induced *E. coli* BL21 (DE3) cells were then cooled on ice for 30 min and harvested by centrifugation at 3500 rpm for 30 min at 4 °C. Harvested cells were resuspended in 20 mL of column buffer (20 mM Tris–HCl pH 7.4 and 200 mM NaCl) and stored at −20 °C. *E. coli* cells were thawed and lysed in column buffer using cold sonication. The protein was then purified using the pMAL™ Protein Fusion and Purification System (New England BioLabs, Ipswich, MA, USA). The purified protein was eluted using an elution buffer (10 mM maltose in column buffer). Its concentration was determined using the Bradford method using bovine serum albumin as the standard (Bradford, 1976). Next, the rRbFerH-MBP fusion product was cleaved using Factor Xa, according to the pMAL™ Protein Fusion and Purification kit protocol. The resultant cleaved protein (rRbFerH) was assayed for its iron(II) depriving, antibacterial, and oxidative DNA damage protection activities. Samples collected at different steps of the rRbFerH purification were analyzed by reducing 12% sodium dodecyl sulfate polyacrylamide gel electrophoresis (SDS–PAGE) using standard protein size markers (Enzynomics, Korea). The gel was stained with 0.05% Coomassie blue R-250, followed by a standard destaining procedure. In addition, to analyze the purified rRbFerH under native conditions, rRbFerH was analyzed by non-reducing native-PAGE using apoferritin from equine spleen (Sigma – USA) as a marker.

### 2.3. Iron(II) depriving activity of rRbFerH

The iron(II) depriving activity of rRbFerH was determined using a previously published method with some modifications (De Zoysa and Lee, 2007). Briefly, 20 μL of 2 mM $FeSO_4$ was added to 1 mL of the recombinant protein diluted to different concentrations in column buffer. Samples were incubated at room temperature (25 °C) for 10 min. To each sample, 5 mM ferrozine (Sigma, USA) was added. Samples were mixed thoroughly and incubated again at room temperature for 15 min. The optical density (OD) of each sample was measured at 562 nm by using a spectrophotometer. To investigate the effect of MBP in the cleaved recombinant fusion protein samples, corresponding concentrations of Factor Xa-cleaved recombinant MBP were used as controls. Each assay was performed in triplicate and the mean OD value was used to calculate the percentage of Fe(II) deprivation. Moreover, in order to determine whether the ferroxidase center in rRbFerH is active, the above assay was repeated in triplicates using 25 μg of rRbFerH (~0.02 μg/μL) under reducing conditions. Therein, reducing medium was produced by the addition of Tin (II) ions (~0.16 M) into the reaction medium as a potent reducing agent of Fe (III) ions possibly formed by the ferroxidase activity of rRbFerH, after the first incubation at room temperature and again incubated for 5 min after the addition of Tin (II) into the medium, before addition of ferrozine into the final reaction medium. Finally, the $OD_{562}$ values obtained for the Fe(II)–ferrozine complex formed in this reaction setup and that of non-reducing conditions (without tin (II)) were compared with the OD values detected for the control (reaction setups without rRbFerH) to calculate the percentage Fe(II) deprivation.

### 2.4. Antibacterial activity of rRbFerH

To analyze the effect of RbFerH on *E. coli* (DH5α) bacterial growth, we measured *E. coli* cell density in liquid culture media at various time points after treating the culture with purified rRbFerH. Bacteria were cultured initially in LB medium at 37 °C until they reached the exponential phase. Cultures were then diluted in fresh LB medium to ~$10^4$ CFU/mL. Diluted cultures were separated into three aliquots (170 mL each). To one of the three aliquots, rRbFerH (50 μg/mL), recombinant MBP (50 μg/mL), or column buffer was added. Aliquots were distributed into the wells of a 96-well cell culture plate. Plates were incubated at 37 °C and cell densities were analyzed by measuring $OD_{600}$ at different time points post-incubation. The assay was carried out in triplicate and the mean $OD_{600}$ reading at corresponding time points was used as the net OD value.

### 2.5. Determination of the effect of rRbFerH on oxidative damage of DNA

We evaluated the effect of rRbFerH on DNA strand breakage under conditions of oxidative stress. The conversion of supercoiled plasmid DNA to nicked (circular) form DNA was measured in solutions containing Fe(II) ions and $H_2O_2$ in the presence and absence of rRbFerH as described previously (Kang, 2010), but with some modifications. Briefly, rRbFerH was added separately into the Fe(II)-containing (0.33 mM) column buffer to achieve a final concentrations of approximately 0.4 and 0.8 μg/μL in a total volume of 45 μL. The mixtures were then incubated at room temperature for 15 min. Subsequently, pUC19 plasmid DNA (2 μg) and $H_2O_2$ (final concentration of ~2.86 mM) were added. Reactions were incubated at 37 °C for 10 min to induce DNA breakage through the formation of hydroxyl radicals from the reaction of Fe(II) and $H_2O_2$. Factor Xa-treated recombinant MBP (final concentration of 0.8 μg/μL) was used in one parallel assay in place of rRbFerH as a control. Another control assay was performed using an equal volume of column buffer without protein. Immediately after incuba-

tion, DNA in each reaction mixture was purified using the Expin™ PCR SV kit (GeneAll., Korea) according to manufacturer's instructions, thus terminating the DNA cleavage reactions. The purified DNA was eluted using 30 μL of DNA elution buffer and the total volume was loaded onto a 1% agarose gel and analyzed by electrophoresis. Bands were compared to undigested pure pUC19 vector DNA. The assay was repeated three times to confirm the reliability of results.

### 2.6. Experimental fish and tissue collection

Healthy rock bream with an average body weight of 50 g were obtained from the Jeju Special Self-Governing Province Ocean and Fisheries Research Institute (Jeju, Republic of Korea). Animals were acclimatized for 1 week prior to the experiment in a controlled environment (34 ± 1 practical salinity units, pH 7.6 ± 0.5, and 22–24 °C). Fish used for tissue collection were maintained in 400 L tanks and fed a commercially available fish feed. Whole blood (1 mL/fish) was collected from the caudal fin by using a sterilized syringe. The samples were immediately centrifuged at 3000*g* for 10 min at 4 °C to separate the blood cells from the plasma. The collected cells were snap-frozen in liquid nitrogen. Fish were sacrificed, and the gill, liver, skin, spleen, head kidney, kidney, heart, muscle, brain, and intestine were excised. Tissues were snap-frozen in liquid nitrogen and stored at −80 °C until they were used for total RNA extraction.

### 2.7. Immune challenge experiments

In time-course immune challenge experiments, we investigated the transcriptional regulation of *RbFerH* in response to pathogenic infection by *Edwardsiella tarda* and rock bream Iridovirus (RBIV), and immune stimulation elicited by lipopolysaccharides (LPS) and polyinosinic:polycytidylic acid (Poly I:C). *E. tarda* was obtained from the Department of Aqualife Medicine, Chonnam National University, Korea. The bacteria were incubated at 25 °C for 12 h in brain–heart infusion broth (Eiken Chemical Co., Japan) supplemented with 1% sodium chloride. The cultures were resuspended in sterile phosphate-buffered saline (PBS) and diluted to the desired concentration ($1 \times 10^5$/mL) for injection. For the virus challenge experiment, kidney tissue specimens were obtained from moribund rock bream infected with RBIV and homogenized in 20 volumes of PBS. Tissue samples were centrifuged at 3000*g* for 10 min at 4 °C to obtain the RBIV containing supernatants. Supernatants were filtered through a 0.45 μm membrane and injected into the fish. LPS (*E. coli* 055:B5, Sigma) was resuspended in sterilized PBS to reach the desired concentration for injection. The immune challenge experiments were performed as previously described (Whang et al., 2011b). Tissues were collected from at least 3 animals from each challenge group at each time point. Tissues were collected as described in Section 2.6.

### 2.8. Total RNA extraction and cDNA synthesis

Using Tri Reagent™ (Sigma), total RNA was extracted from the blood, gill, liver, spleen, head kidney, kidney, brain, skin, muscle, intestine, and brain tissues from healthy rock breams, as well as from blood cells collected from immune-challenged animals; subsequently cDNA was synthesized from each total RNA as previously described (Whang et al., 2011a).

### 2.9. RbFerH transcriptional analysis by quantitative real-time PCR

Quantitative real-time PCR (qPCR) was used to analyze the expression levels of *RbFerH* in the blood, gill, liver, spleen, head kidney, kidney, skin, muscle, brain, and intestine tissues of healthy fish. The temporal expression of *RbFerH* in liver tissues of immune-challenged animals was also measured using qPCR. Total RNA was extracted at different time points following the respective immune challenges, and first-strand cDNA synthesis was performed as described in Section 2.8. qPCR was performed using the Dice™ Real-Time System thermal cycler (TP800; TaKaRa, Japan) in a 15 μL reaction volume containing 4 μL of diluted cDNA from each tissue, 7.5 μL of 2× TaKaRa ExTaq™ SYBR premix, 0.6 μL of each primer (RbFerH-qF and RbFerH-qR; Table 1), and 2.3 μL of $ddH_2O$ as per the essential MIQE guidelines (Bustin et al., 2009). qPCR analysis was performed under the following conditions: 95 °C for 10 s; 35 cycles of 95 °C for 5 s, 58 °C for 10 s, and 72 °C for 20 s; and a final cycle of 95 °C for 15 s, 60 °C for 30 s, and 95 °C for 15 s. The baseline was set automatically by the Dice™ Real Time System software (version 2.00). *RbFerH* expression was determined using the Livak ($2^{-\Delta\Delta CT}$) method (Livak and Schmittgen, 2001). The same qPCR cycle profile parameters were used for the internal control gene, rock bream β-actin (GenBank ID: FJ975145). The primers used for the control gene are listed in Table 1. No tissue-specific difference in β-actin expression was observed under these experimental conditions. The data are presented as the mean ± standard deviation (SD) of the relative mRNA expression in experiments performed in triplicate. To determine statistical significance ($P < 0.05$) between the experimental and control groups, two-tailed un-paired Student's *t*-tests were performed. In immune challenge experiments, the expression levels of *RbFerH* mRNA relative to that of the rock bream β-actin gene were calculated. Values were further normalized to the corresponding PBS-injected controls at each time point. The relative expression level in the uninjected control at the 0-h time point was used as the baseline reference.

## 3. Results and discussion

### 3.1. Sequence profiles and homology

The *in silico* analysis of the identified cDNA sequence (1151 bp) showed that *RbFerH* consisted of a 531 bp coding sequence flanked by 307 bp 5′ and 313 bp 3′ untranslated regions (UTRs). Resembling the typical characteristics of ferritin H subunits, the 5′ UTR of *RbFerH* bears an iron response element (IRE – $^{48}$TTACCTGCTTCAACAGTGCT TGAACGGCAA$^{77}$), which is important to regulate its expression depending on the availability of Fe(II) in the cellular environment (Thomson et al., 1999). The deduced amino acid sequence of RbFerH consisted of 177 amino acids. We calculated the molecular mass to be ~20.8 kDa and the theoretical isoelectric point was 5.56. The amino acid sequence of RbFerH possessed the characteristic domain architecture of ferritin H, including two iron-binding region signatures ($^{58}$EEREHAEKLMKLQNQRGGR$^{76}$ and $^{123}$DPHLCDFIETH YLDEQVK$^{140}$) and seven putative amino acid residues that comprise the ferroxidase center (E-24, Y-31, E-58, E-59, H-62, E-104, and Q-138) (Fig. 1).

The sequencing results showed that the *RbFerH* gene was 4195 nucleotides in length and split into 5 exons separated by 4 introns (Fig. 2). As shown in Fig. 2, orthologs from the other teleosts examined had five exons, suggesting they had similar genomic architecture. The size of the internal exons 2–4 (flanked by the first and last introns) and the coding region of the last exon were found to be highly conserved. Notably, the 5′ UTR of *RbFerH* was split between two exons, a feature common to the genomic gene architectures of the other teleost species examined. The genomic organizations of teleost ferritin H genes were dramatically different compared to that of the higher vertebrates (mammals and birds). In this regard ferritin H genes belonging to mammals (human and mouse) and birds (chicken) contained only 4 exons, with the coding region

starting on the first exon, while the teleost genes consisted of 5 exons. Therefore, we speculate that one intron was lost from the ferritin H genes of teleosts or single intron was acquired by teleostan counterparts at the divergence of the lower and higher vertebrates. Nevertheless, a loss of an intron likely trim down the functional diversity of ferritin H through reducing the number of variants generated by alternative splicing, while potentially increasing the rate of the gene evolution (Keren et al., 2010; Parmley et al., 2007) or *vice versa*. However, further studies on molecular evolutionary aspects of ferritin H should be carried out to draw clear conclusions on this observation. The sizes of exons 2 and 3 of the higher vertebrate ferritin H orthologs were observed to be identical to that of exons 3 and 4 of the teleost orthologs including *RbFerH*. These conserved exons may represent functionally important regions in the coding sequence of ferritins.

Identity and similarity analysis of RbFerH with its homologues was performed using pairwise sequence alignments. RbFerH shared clear homology with vertebrate ferritin H orthologs and substantial homology with ferritin M orthologs, which are known to possess properties similar to ferritin H subunits (Table 2). The ferritin H subunit of the European sea bass (*D. labrax*) showed the greatest percent sequence similarity and identity to RbFerH. On the other hand, RbFerH shared relatively low sequence similarity to the ferritin L orthologs included in the analysis, affirming the distant relationship between two subunit genes. Multiple sequence alignment of RbFerH with its vertebrate orthologs revealed that the seven amino acid residues of RbFerH that bind iron and form the ferroxidase center are conserved among all the orthologs examined. These data can partially validate that RbFerH is a homolog of the vertebrate ferritin H subunit (Fig. 1).

### 3.2. Phylogenetic relationship of RbFerH

A phylogenetic reconstruction of RbFerH and its homologs showed that the three ferritin subunits, H, L and M, formed three distinct clusters which grouped closely and independently (Fig. 3). The ferritin H subunit cluster was further divided into mammalian, avian, and piscine clades. The orthologs belonging to the marine teleosts were diverged from their fresh water teleost counterparts, represented by zebrafish ferritin H. With strong bootstrapping support (86), RbFerH was grouped within the ferritin H sub-clade formed by the orthologs of sea bass and large yellow croaker, supporting its homology to teleost ferritin H orthologs. RbFerH was observed to have a distant evolutionary relationship with vertebrate L and M subunits, as evidenced by their distinctive clustering patterns. Moreover, our tree predicts that teleosts possess H and M ferritin subunits, whereas mammals are more likely have H and L subunits. These data suggest that ferritin H is likely to be the common ancestral type of ferritin subunits. In addition, the H subunit of the fruit fly, the sole invertebrate ortholog included

```
Sea bass                ----MSSQVRQNFHQDCEAAINRQINLELYASYVYLSMAYYFDRDDQALHNFAKFFRNQS 56
Large yellow croaker    ----MSSQVRQNFHQDCEAAVNRQINLELYASYVYLSMAYYFDRDDQALHNFAKFFRNQS 56
Rock bream              ----MSSQVRQNFHQDCEAAINRQINLELYASYVYLSMAYYFDRDDQALHNFAKFFRNQS 56
Orange-spotted grouper  ----MSSQVRQNYHQDCEAAINRQINLELYASYVYLSMGYYFDRDDQALHNFAKFFRHQS 56
Zebrafish               ----MSSQVRQNFEEACEAAVNRQINMELYASYVYLSMSYYFDRDDQALHNFAKFFRHQS 56
Human                   MTTASTSQVRQNYHQDSEAAINRQINLELYASYVYLSMSYYFDRDDVALKNFAKYFLHQS 60
Mouse                   MTTASPSQVRQNYHQDAEAAINRQINLELYASYVYLSMSCYFDRDDVALKNFAKYFLHQS 60
Chicken                 MATP-PSQVRQNYHQDCEAAINRQINLELYASYVYLSMSYYFDRDDVALKNFAKYFLHQS 59
Frog                    ----MNSQIRQNFHQECEAAINRQVNMELYASYVYLSMSYYFDRDDVALKNFAKYFLHQS 56
                              ** ***     *** *** * ***********  ****** ** **** *  **

Sea bass                QEEREHAEKLMKVQNQRGGRIFLQDIRKPERDEWGSGIEALECALQLEKSVNQSLLDMHK 116
Large yellow croaker    QEEREHAEKLMKLQNQRGGRIFLQDIRKPERDEWGSGIEALECALQLEKSVNQSLLDMHK 116
Rock bream              HEEREHAEKLMKLQNQRGGRIFLQDVRKPERDEWGSGIEALECALQLEKSVNQSLLDLHK 116
Orange-spotted grouper  HEEREHAEKLMKLQNQRGGRIFLQDVKKPERDEWGSGVEALECALQLEKSVNQSLLDLHK 116
Zebrafish               HEEREHAEKLMKFQNQRGGRIFLQDVKKPEKDEWGSGVEALECALQLEKSVNHSLLELHK 116
Human                   HEEREHAEKLMKLQNQRGGRIFLQDIKKPDCDDWESGLNAMECALHLEKNVNQSLLELHK 120
Mouse                   HEEREHAEKLMKLQNQRGGRIFLQDIKKPDRDDWESGLNAMECALHLEKSVNQSLLELHK 120
Chicken                 HEEREHAEKLMKLQNQRGGRIFLQDIKKPDRDDWENGLTAMECALHLEKNVNQSLLELHK 119
Frog                    HEEREHAEKLMKMQNQRGGRLFLQDIKKPERDEWANGLEALECSLQLEKNVNQSLLELHK 116
                         *********** ******* ****  **  * *  *  * ** * *** ** ***  **

Sea bass                LCSDHNDPHLCDFIETHYLDEQVKSIKELADWVTNLRRMGAPQNGMAEYLFDKHTLGKES 176
Large yellow croaker    LCSDHNDPHMCDFIETHYLDEQVKSIKELADWVTNLRRMGAPQNGMAEYLFDKHTLGKES 176
Rock bream              LCSDHNDPHLCDFIETHYLDEQVKSIKELADWVTNLRRMGAPQNGMAEYLFDKHTLGKES 176
Orange-spotted grouper  LCSEHNDPHLCDFIETHYLDEQVKSIKELADWVTNLRRMGAPQNGLAEYLFDKHTMGKES 176
Zebrafish               LASQHNDPHMCDFIETHYLDEQVKSIKELGDHVTNLRRMGAPQNGMAEYMFDKLTLGKES 176
Human                   LATDKNDPHLCDFIETHYLNEQVKAIKELGDHVTNLRKMGAPESGLAEYLFDKHTLGDSD 180
Mouse                   LATDKNDPHLCDFIETYYLSEQVKSIKELGDHVTNLRKMGAPEAGMAEYLFDKHTLGHGD 180
Chicken                 LATEKNDPHLCDFIETHYLDEQVKAIKQLGDHVTNLRKMGAPKYGMAEYLFDKHTLGESD 179
Frog                    LSTDHNDPHLCDFLESHYLDEQVKSMKELGDHITNLRRMGAPSNGLAEYLFDKHTLGEDH 176
                        *    **** *** *  ** ****  * * *  **** ****  * *** *** * *

Sea bass                 S-- 177
Large yellow croaker     S-- 177
Rock bream               S-- 177
Orange-spotted grouper   S-- 177
Zebrafish                S-- 177
Human                    NES 183
Mouse                    -ES 182
Chicken                  --S 180
Frog                     E-- 177
```

**Fig. 1.** Multiple sequence alignment of vertebrate ferritin H subunit orthologs including rock bream ferritin H (RbFerH). Two putative iron-binding region signatures of RbFerH are indicated by the double underline. Conserved residues involved in iron binding and the formation of the ferroxidase center are shaded in gray. Residues conserved in all the aligned sequences are denoted by asterisks (*).

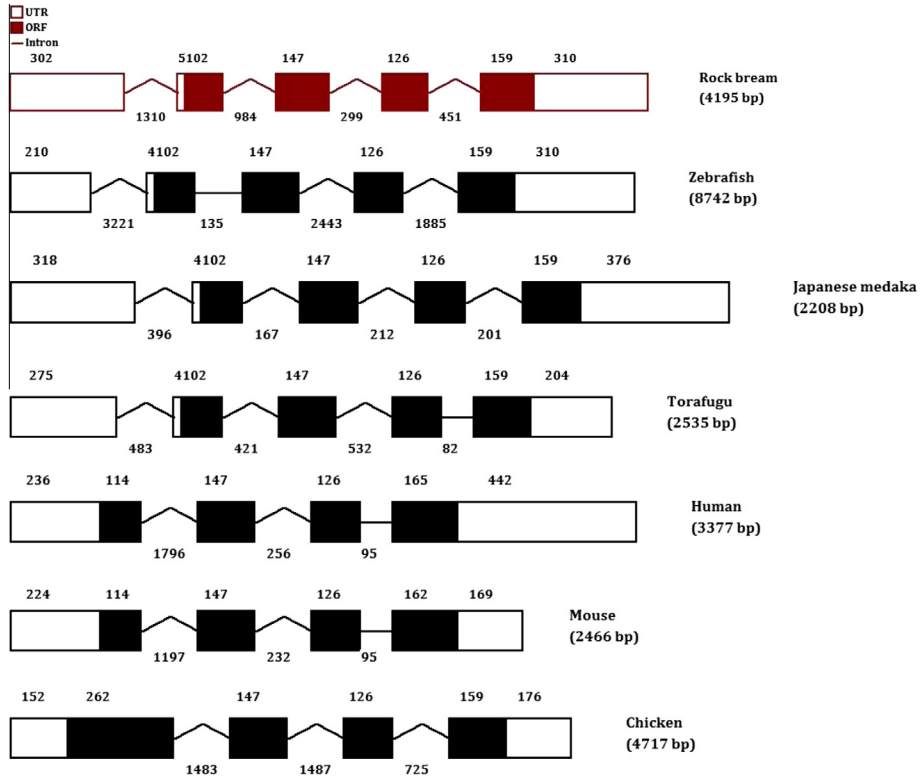


**Fig. 2.** Exon–intron arrangement of the RbFerH gene and its orthologs from other vertebrate species. Introns greater than 150 bp are indicated by peaked lines. The intron and exon lengths are indicated above and below each structure, respectively. The genomic DNA sequence information for each ortholog was obtained from the National Center for Biotechnology Information (NCBI) GenBank database. The NCBI gene ID numbers as follows: zebrafish, 18858718; Japanese medaka, 101169025; torafugu, 101064331; human, 2495; mouse, 14391; and chicken, 395970.

**Table 2**
Percentage similarity and identity values of RbFerH with its orthologs.

| Species name | Subunit type | NCBI accession number | Amino acids | Identity | Similarity |
|---|---|---|---|---|---|
| 1. European seabass (*Dicentrarchus labrax*) | H | ACN80998 | 177 | 97.7 | 99.4 |
| 2. *Larimichthys crocea* (Large yellow croaker) | H | ACY75475 | 177 | 97.2 | 99.4 |
| 3. *Anoplopoma fimbria* (Sablefish) | H | ACQ59065 | 177 | 97.2 | 98.9 |
| 4. *Epinephelus coioides* (Orange-spotted grouper) | H | AEG78374 | 177 | 95.5 | 99.4 |
| 5. *Salmo salar* (Atlantic salmon) | H | NP001117129 | 177 | 92.7 | 98.9 |
| 6. *Danio rerio* (Zebrafish) | H | NP571660 | 177 | 88.7 | 94.9 |
| 7. *Xenopus laevis* (Frog) | H | NP001083072 | 182 | 80.2 | 94.4 |
| 8. *Taeniopygia guttata* (Zebra finch) | H | NP001232211 | 180 | 79.4 | 89.4 |
| 9. *Gallus gallus* (Chicken) | H | NP990417 | 180 | 78.9 | 90.0 |
| 10.*Mus musculus* (Mouse) | H | NP034369 | 182 | 78.7 | 86.9 |
| 11.*Cavia porcellus* (Guinea pig) | H | NP001166318 | 182 | 78.6 | 87.9 |
| 12.*Canis lupus familiaris* (Dog) | H | NP001003080 | 183 | 78.1 | 88.0 |
| 13*Anas platyrhynchos* (Mallard) | H | AGD91914 | 181 | 77.9 | 88.4 |
| 14.*Homo sapiens* (Human) | H | NP002023 | 183 | 76.5 | 88.0 |
| 15.*Chionodraco rastrospinosus* (Ice fish) | M | CCO75659 | 176 | 71.3 | 84.8 |
| 16.*Sciaenops ocellatus* (Red drum) | M | ADF80517 | 176 | 70.6 | 86.4 |
| 17.*Homo sapiens* (Human) | L | AAA52439 | 175 | 55.4 | 73.4 |
| 18.*Mus musculus* (Mouse) | L | NP034370 | 183 | 53.0 | 71.4 |
| 19.*Drosophila melanogaster* (Fruit fly) | H | NP524873 | 205 | 29.2 | 40.6 |

in the tree construction, was clearly separated from the main vertebrate cluster, forming an out-group. Taken together, the overall clustering pattern of our phylogenetic reconstruction suggests that RbFerH shares a common ancestral origin with the ferritin subunits of vertebrates, and more specifically with teleosts.

### 3.3. Integrity, purity and degree of ferritin complex formation of rRbFerH

SDS–PAGE analysis showed that the rRbFerH fusion protein was successfully produced using IPTG induction under the experimental conditions (Fig. 4A). A single band was resolved from the sample collected after the protein purification process (lane 4), suggesting that our fusion protein was eluted with high purity and was intact (Fig. 4A). The fusion protein was approximately 63 kDa in size, correlating with the predicted molecular mass of RbFerH (20.8 kDa) and MBP (42.5 kDa). After treatment with Factor Xa, the fusion protein was successfully cleaved into rRbFerH and MBP, as evidenced by the two bands with corresponding molecular masses that resolved in lane 5. Our native-PAGE analysis affirmed that rRbFerH monomers have adequately assembled into ferritin protein complex to form apoferritin (protein nano cage), as detected by the band resolved on the gel (Fig. 4B; lane 2) aligning with the band observed corresponding to the equine apoferritin

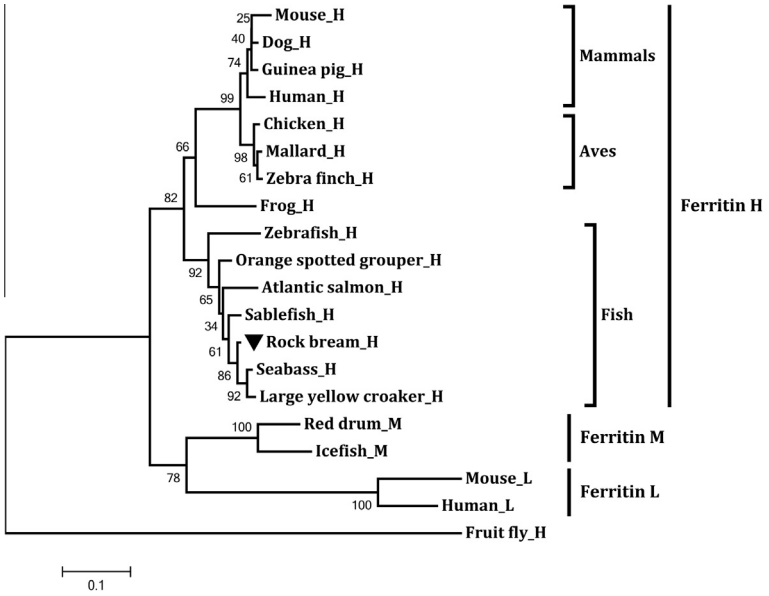


**Fig. 3.** Phylogenetic reconstruction of RbFerH and its orthologs. The evolutionary relationship of the different ferritin subunits was analyzed based on ClustalW alignments of the respective amino acid sequences by using the neighbor-joining function of the MEGA 4.0 software. Corresponding bootstrap values are indicated on nodes of the tree. NCBI GenBank accession numbers of the ferritin H subunit amino acid sequences used in the construction are listed in Table 2.

(Fig. 4B; lane 1). In addition, rest of the bands present in the gel (lane 2) may reflect the monomers as well as oligomers of rRbFerH and cleaved MBP.

### 3.4. Iron(II) depriving activity of rRbFerH

The iron(II) depriving activity of rRbFerH was analyzed using an assay that is based on the principle of OD reduction of the Fe(II)–ferrozine chromogenic complex at 562 nm, due to the binding of free Fe(II) ions by iron binding proteins like ferritins. According to the observed results, rRbFerH was detected to deprive Fe(II) in the medium in a concentration-dependent manner (Fig. 5A). At an rRbFerH concentration of 0.025 μg/μL, the percentage of deprived iron(II) reached its maximum level (~90%). The dose–response curve plateaued at higher concentrations of rRbFerH, suggesting the optimal conditions for the reaction had been attained. However, under reducing conditions, iron(II) deprivation in the final reaction medium was significantly lower (~23%) than that of non-reducing conditions (~87%) with the presence of rRbFerH (Fig. 5B). In general, H subunits of ferritins can demonstrate ferroxidase activity by converting Fe(II) ions into Fe(III) ions in the medium (Lawson et al., 1989), which could be further prefigured regarding rRbFerH, due to the presence of residues for the ferroxidase center, as per our *in silico* prediction. Thus, according to our observation, reducing conditions could compensate the iron(II) deprivation by rRbFerH to a significant extend, suggesting that detectable ferroxidase activity can be demonstrated by rRbFerH, via active ferroxidase center. Notably, the MBP control did not show any significant Fe(II) deprivation at any concentration tested, suggesting that it does not contribute to the prominent ferroxidase activity of rRbFerH.

### 3.5. Antibacterial activity of rRbFerH

Since rRbFerH demonstrated a substantial iron(II) depriving activity (Section 3.4), we evaluated its bacteriostatic activity towards the growth of *E. coli* (DH5α) potentially mediated by iron(II) binding and conversion to the less-soluble and less biologically available form of iron; iron(III) at its ferroxidase center (Krewulak and Vogel, 2008). As shown in Fig. 6, rRbFerH restricted bacterial growth. Bacterial cell density, measured by $OD_{600}$ started to decline 6 h post-rRbFerH treatment compared to that of control culture samples at same time point. In contrast, the bacterial cell density ($OD_{600}$) of MBP-treated cultures elevated gradually, in a manner similar to the control culture sample. Therefore, we could infer that MBP in the rRbFerH solution does not have any detectable antibacterial effect on *E. coli*. The bacteriostatic activity of rRbFerH was likely mediated through the deprivation of Fe(II) ions in the culture medium, reducing the free iron (Fe(II) ions) available for bacterial growth. This may probably due to binding of free Fe(II) ions to the ferroxidase center of rRbFerH apoferritin complex to convert them into less biologically available Fe III (Section 3.4). Moreover, to a lesser extend *E. coli* growth reduction may depends on the depletion of dissolved oxygen in the culture medium, as a result of iron(II) oxidation process at its ferroxidase center.

### 3.6. Protective effect of rRbFerH in oxidative DNA damage

Fe(II) ions are catalysts for the Fenton-type reactions that can damage DNA in cells through the production of radicals using substrates such as $H_2O_2$ (Luo et al., 1996). However, iron binding proteins like ferritins can help to prevent these reactions by reducing the availability of free Fe(II) in cells, in turn preventing oxidative DNA damage. We tested the ability of rRbFerH to protect DNA against the radical formation caused by the reaction between Fe(II) and $H_2O_2$ *in vitro*. In reaction solutions containing Fe(II) and $H_2O_2$, rRbFerH protected pUC19 plasmid DNA from strand breakage, as indicated by the significant reduction in the conversion of supercoiled to nicked DNA (Fig. 7, lanes 4 and 5) relative to the untreated control (Fig. 7, lane 2). The intensity of the DNA band corresponding to the nicked DNA decreased with increasing concentrations of rRbFerH, suggesting its protective effect on DNA breakage was concentration-dependent (Fig. 7, lanes 5 to 4). MBP-treated controls did not show any detectable protection against Fe(II) and $H_2O_2$-mediated DNA damage. In these controls, the majority of the supercoiled DNA was converted into the nicked form, suggesting MBP is inert in the rRbFerH solution. Based on these observations, we speculate that RbFerH prevents the DNA damage induced by

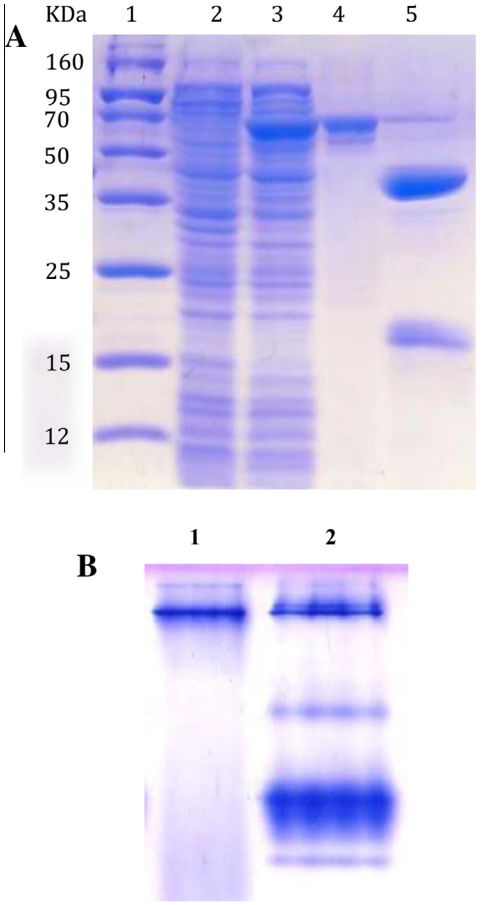


**Fig. 4.** (A) SDS–PAGE analysis of the purified recombinant RbFerH (rRbFerH)-maltose binding protein (MBP) fusion protein and its cleaved products after treatment with Factor Xa. Lane 1, protein size marker; lane 2, total cellular extract from *E. coli* BL21 (DE3) carrying the rRbFerH-MBP expression vector prior to IPTG induction; lane 3, crude extract of rRbFerH after IPTG induction; lane 4, purified recombinant fusion protein (rRbFerH-MBP) after IPTG induction (1 mM); lane 5, cleaved products (MBP and rRbFerH) of the rRbFerH fusion protein after treatment with Factor Xa; (B) Non reducing, native PAGE analysis of Factor Xa cleaved rRbFerH. Lane 1, apoferritin from equine spleen (Sigma) as a marker and lane 2, Factor Xa cleaved rRbFerH.

Fenton-type reactions, probably due to the binding of Fe(II) ions to the active ferroxidase center of RbFerH apoferritin complex (Section 3.4), thereby restricting free iron(II) availability. Therefore, RbFerH may play an indirect role in cellular antioxidative defense.

### 3.7. Spatial expression pattern of RbFerH

*RbFerH* was found to be expressed ubiquitously in the tissues examined, indicating its vital function in rock bream physiology. From the tissues examined, the liver and blood tissues showed the highest level of expression (Fig. 8). Interestingly, these data are consistent with previous studies reporting high-level expression of ferritin H in the livers of the Atlantic salmon (*S. salar*) (Andersen et al., 1995), Antarctic notothenioids (Scudiero et al., 2007), catfish (Liu et al., 2010), and sea bass (Neves et al., 2009). The ferritin H ortholog identified in turbot, on the other hand, is highly expressed in muscle tissue and moderately expressed in liver tissues (Zheng et al., 2010b). In contrast to teleost ferritin H expression, mammalian orthologs of ferritin H are expressed predominantly in the heart and brain.

The liver acts as a key mediator of iron metabolism and iron storage (Anderson and Frazer, 2005; Graham et al., 2007). Moreover, the liver functions in the first line host defense because

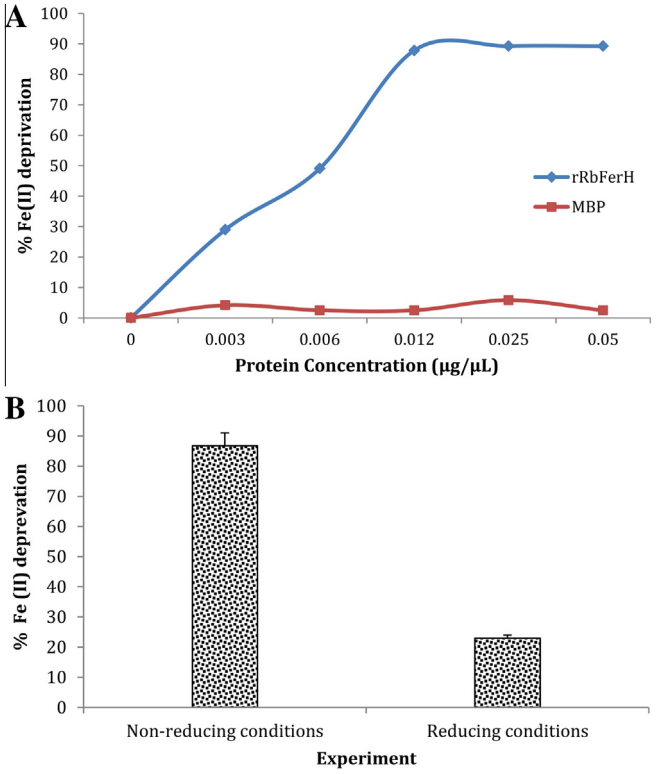


**Fig. 5.** (A) *In vitro* iron(II) deprivation by rRbFerH. The percentage of Fe(II) deprivation is shown for different concentrations of rRbFerH. Error bars represent standard deviation (SD; $n = 3$). The percentage of Fe(II) deprivation was calculated from $OD_{562}$ values measured 10 min after adding ferrozine to the mixture of $FeSO_4$ containing different concentrations of rRbFerH. (B) The percentage Fe(II) deprivation for 0.2 µg/µL of rRbFerH under reducing (with Tin(II) ions) and non-reducing (without Tin(II) ions) conditions. Error bars represent standard deviation (SD; $n = 3$).

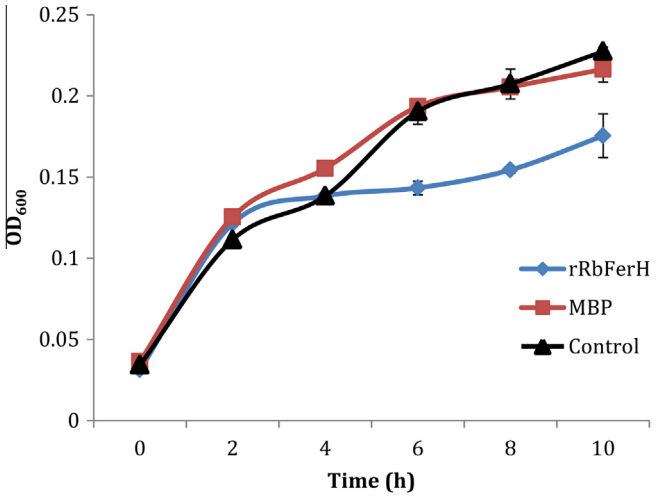


**Fig. 6.** Bacteriostatic activity of rRbFerH, as measured by the effect of rRbFerH (50 µg/mL) on *E. coli* in LB medium. $OD_{600}$ was measured to determine the cell density of *E. coli* in the presence of rRbFerH or MBP, or in the absence of both proteins at different time points. Error bars represent SD ($n = 3$).

it houses different immune-related cell types including Kupffer and natural killer cells (Seki et al., 2000). Thus, we anticipated the prominent expression of RbFerH-like subunits of ferritin important in formation of its apoferritin-complex in the liver because of the involvement of ferritins in iron metabolism, storage (Watt, 2011), and acute phase inflammatory reactions (Worwood, 1990). The liver is an organ in which a wide array of metabolic

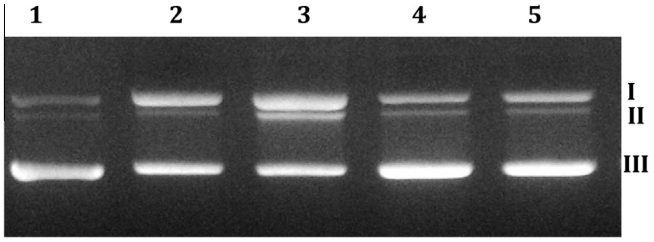


**Fig. 7.** Protective effect of rRbFerH on oxidative damage to dsDNA. Supercoiled pUC19 DNA was converted into a nicked form due to $H_2O_2$ and Fe(II)-mediated radical formation. The effect of rRbFerH on this process was assessed. The reaction mixtures were analyzed by agarose gel electrophoresis to determine the degree of DNA breakage. Lane 1, pUC19 plasmid DNA alone; lane 2, reaction mixture without the addition of rRbFerH (untreated); lane 3, reaction mixture treated with 50 μg of MBP; lane 4, reaction mixture treated with 50 μg of rRbFerH; and lane 5, reaction mixture treated with 25 μg of rRbFerH.

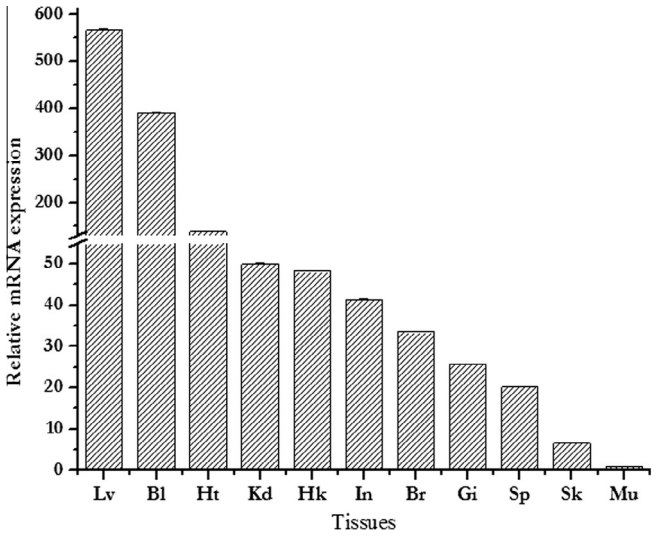


**Fig. 8.** Tissue-specific distribution of *RbFerH* expression in rock bream measured using quantitative real-time polymerase chain reaction (qPCR). Fold-changes in expression are shown relative to the mRNA expression level in muscle tissue. Error bars represent SD ($n = 3$). Lv – liver, Bl – Blood, Ht – Heart, Kd – Kidney, Hk – Head Kidney, In – Intestine, Br – brain, Gi – Gill, Sp – Spleen, Sk – Skin and Mu – Muscle.

reactions occurs. In turn, these metabolic reactions generate ROS such as peroxides. In Section 3.6, we demonstrated that RbFerH reduced the production of radicals generated by Fenton-type reactions using peroxides as the substrate. This may also explain the pronounced expression of *RbFerH* in liver tissues. Because blood cells are involved in first line host defense against invading pathogens, the prominent expression of *RbFerH* in the blood can be attributed to the involvement of ferritins in acute-phase reactions (Worwood, 1990) and its potent antimicrobial activity (Ong et al., 2006). Blood cells such as macrophages store iron after erythrophagocytosis and this iron is then liberated it in response to regulation by proteins involved in iron metabolism, including ferritins (Hausmann et al., 1976; Knutson et al., 2005). Therefore, the abundant expression of prominent ferritin constituents, such as *RbFerH*, in rock bream blood tissue is not unexpected.

### 3.8. Transcriptional modulation of RbFerH expression upon immune stimulation

To decipher the potential role of RbFerH in host immune defense under conditions of pathogenic stress, we analyzed the temporal transcriptional regulation of *RbFerH* in blood tissue after stimulating healthy fish with live pathogens (*E. tarda*, RBIV) and pathogen-derived mitogens (Poly I:C and LPS). As expected, upon stimulation with bacterial stimulants (LPS and *E. tarda*), a significant ($P < 0.05$) increase in *RbFerH* transcription was detected, albeit with a relatively low fold-difference (Fig. 9A). Under conditions of LPS stimulation, *RbFerH* basal transcription was significantly elevated during the early phase (3 h and 6 h) post-stimulation (p.s.). In contrast, *E. tarda*, a common Gram-negative bacterial pathogen of fish induced transcription at a slightly later time point (6 h and 12 h p.s.). However, both stimulants triggered a similar pattern of transcriptional response. In both groups, the *RbFerH* transcript returned to basal levels, suggesting that LPS and *E. tarda* exerted the same immunogenic effects irrespective to their strength of induction. Notably, LPS is a well-known endotoxin of Gram-negative bacteria such as *E. tarda*. Ultimately, this immune stimulation might have elevated *RbFerH* expression to form its apoprotein, in turn suppressing bacterial proliferation in cellular environments through an iron-sequestering strategy (Ong et al., 2006). On the other hand, the observed inductive transcriptional responses of *RbFerH* may also be a secondary response to control the production of reactive oxygen or nitrogen intermediates trigged by the bacterial invasion or LPS stimulation by the host first line immune defense system (Wink et al., 2011), by elevating the ferritin complex formation to withhold iron(II) (Ong et al., 2006), in turn regulating the oxidative stress of the cells elicited by Fenton type reactions (Crichton et al., 2002).

Transcriptional upregulation of the ferritin H subunit gene upon bacterial invasion was also detected in other fish species including

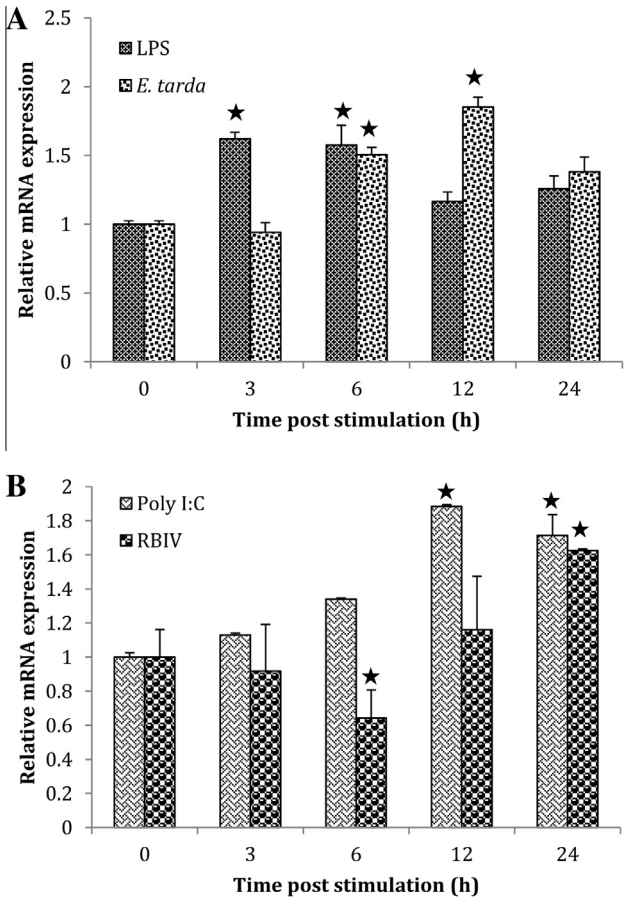


**Fig. 9.** Temporal regulation of *RbFerH* transcription in blood tissue upon immune stimulation with (A) lipopolysaccharides (LPS) and *E. tarda*, and (B) polyinosinic:polycytidylic acid (poly I:C) and rock bream Iridovirus (RBIV), as measured using qPCR. The relative expression was calculated using the $2^{-\Delta\Delta CT}$ method. Rock bream β-actin was used as the reference gene in the corresponding PBS-injected controls at each time point. The relative fold-change in expression at 0 h post-injection was used as the baseline. Error bars represent SD ($n = 3$); ★ $P < 0.05$.

catfish (Liu et al., 2010), sea bass (Neves et al., 2009), and turbot (Zheng et al., 2010b). In the case of catfish, treatment with *Edwardsiella ictaluri* and iron dextran elevates the transcriptional level of ferritin H at 4 h and 7 d post-treatment in liver tissues. The late-phase elevation (7 d) was presumed to be the response induced by the bacterial pathogen. On the other hand, a bacterium known as *Photobacterium damselae* triggers a significant transcriptional induction of the ferritin H subunit gene in the liver and brain tissues of sea bass at two time points (72 h and 96 h) and three time points (48 h, 72 h, and 96 h) p.s., respectively. Upon the exposure to *Listonella anguillarum*, *E. tarda*, or *Streptococcus iniae*, the transcript levels of turbot ferritin H are positively regulated at several time points post-exposure, showing prominent fold-changes compared to its basal level of transcription.

Providing the first insights into the transcriptional regulation of the ferritin H subunit in fish upon live viral infection, we showed that the expression of *RbFerH* was significantly ($P < 0.05$) induced by RBIV invasion in blood cells during the late phase p.s. (24 h p.s.; Fig. 8B). ROS are reportedly generated to induce apoptosis in cells as a host antiviral defense strategy (Skulachev, 1998). To regulate the excessive ROS produced by Fenton-type reactions (Crichton et al., 2002), ferritin may have an indispensible role in binding free Fe(II) ions. This is in accordance with our observation that the transcriptional response of *RbFerH* is induced upon RBIV infection. At 6 h p.s., *RbFerH* transcript levels were diminished, probably due to an immune evasion mechanism orchestrated by RBIV. Immune evasion mechanisms are typical of other viral pathogens of vertebrate host species (Iannello et al., 2005). Plausibly, this stimulates ROS production in host blood cells. A number of viral pathogens are known to maintain their presence by promoting the spread of virions through destroying host cells by using virus-induced ROS generation (Yang et al., 2010). Treatment with poly I:C, a well-known double-stranded viral RNA analog significantly ($P < 0.05$) increased the basal transcription of *RbFerH* during the late phase of the experiment (12 h and 24 h p.s.). This result is consistent with that of a previous report in turbot (Zheng et al., 2010b). Poly I:C treatment in turbot also triggers an inductive transcriptional response during the late phase post-treatment and relatively high fold-changes. The distinct patterns of the transcriptional responses elicited by two different viral stimuli may be attributed to the induction of two different immune pathways that ultimately regulate the expression of *RbFerH*. Taken together, the transcriptional regulation of *RbFerH* under conditions of pathogenic stress suggests that RbFerH plays an important role in the host antimicrobial defense system. This is supported by the prominent antibacterial activity of RbFerH *in vitro* (Section 3.5).

## 4. Conclusion

The results of this study revealed that RbFerH shared significant features of typical vertebrate H ferritins and it is transcribed in tissue-specific manner, with prominent expression levels in blood and liver tissues. Moreover, *RbFerH* expression in blood tissue is regulated by pathogen infection. Analyses of RbFerH functionality indicated its potential participation in antibacterial and antioxidative defense, probably through its iron-sequestering properties. Based on these data, we identify RbFerH as a major factor involved in multiple biological functions, including regulatory functions related to rock bream physiology.

## Acknowledgment

This research was a part of the project titled 'Development of Fish Vaccines and Human Resource Training', funded by the Ministry of Oceans and Fisheries, Korea.

## References

Alkhateeb, A.A., Connor, J.R., 2010. Nuclear ferritin: A new role for ferritin in cell biology. Biochim. Biophys. Acta 1800, 793–797.
Andersen, O., Dehli, A., Standal, H., Giskegjerde, T.A., Karstensen, R., Rørvik, K.A., 1995. Two ferritin subunits of Atlantic salmon (*Salmo salar*): cloning of the liver cDNAs and antibody preparation. Mol. Mar. Biol. Biotechnol. 4, 164–170.
Anderson, G.J., Frazer, D.M., 2005. Hepatic iron metabolism. Semin. Liver Dis. 25, 420–432.
Andrews, S.C., Arosio, P., Bottke, W., Briat, J., von Darl, M., Harrison, P.M., Laulhère, J.P., Levi, S., Lobreaux, S., Yewdall, S.J., 1992. Structure, function, and evolution of ferritins. J. Inorg. Biochem. 47, 161–174.
Arosio, P., Ingrassia, R., Cavadini, P., 2009. Ferritins: a family of molecules for iron storage, antioxidation and more. Biochim. Biophys. Acta 1790, 589–599.
Arosio, P., Yokota, M., Drysdale, J.W., 1976. Structural and immunological relationships of isoferritins in normal and malignant cells. Cancer Res. 36, 1735–1739.
Bradford, M.M., 1976. A rapid and sensitive method for the quantitation of microgram quantities of protein utilizing the principle of protein-dye binding. Anal. Biochem. 72, 248–254.
Bustin, S.A., Benes, V., Garson, J.A., Hellemans, J., Huggett, J., Kubista, M., Mueller, R., Nolan, T., Pfaffl, M.W., Shipley, G.L., Whang, I., 2009. The MIQE guidelines: minimum information for publication of quantitative real-time PCR experiments. Clin. Chem. 55, 611–622.
Caskey, J.H., Jones, C., Miller, Y.E., Seligman, P.A., 1983. Human ferritin gene is assigned to chromosome 19. Proc. Natl. Acad. Sci. U.S.A. 80, 482–486.
Coffman, L.G., Brown, J.C., Johnson, D.A., Parthasarathy, N., D'Agostino, R.B.J., Lively, M.O., Hua, X., Tilley, S.L., 2008. Cleavage of high-molecular-weight kininogen by elastase and tryptase is inhibited by ferritin. Am. J. Physiol. Lung Cell. Mol. Physiol. 294, L505–L515.
Crichton, R.R., Declercq, J.P., 2010. X-ray structures of ferritins and related proteins. Biochim. Biophys. Acta 1800, 706–718.
Crichton, R.R., Wilmet, S., Legssyer, R., Ward, R.J., 2002. Molecular and cellular mechanisms of iron homeostasis and toxicity in mammalian cells. J. Inorg. Biochem. 91, 9–18.
De Zoysa, M., Lee, J., 2007. Two ferritin subunits from disk abalone (*Haliotis discus discus*): cloning, characterization and expression analysis. Fish Shellfish Immunol. 23, 624–635.
Dickey, L.F., Sreedharan, S., Theil, E.C., Didsbury, J.R., Wang, Y.H., Kaufman, R.E., 1987. Differences in the regulation of messenger RNA for housekeeping and specialized-cell ferritin. A comparison of three distinct ferritin complementary DNAs, the corresponding subunits, and identification of the first processed in amphibia. J. Biol. Chem. 262, 7901–7907.
Do, J., Moon, C., Kim, H.J., Ko, M.S., Kim, S.B., Son, J.H., Kim, J.S., An, E.J., Kim, M.K., 2004. Complete genomic DNA sequence of rock bream iridovirus. Virology 325, 351–363.
Elvitigala, D.A., Premachandra, H.K., Whang, I., Oh, M.J., Jung, S.J., Park, C.J., Lee, J., 2013. A teleostean counterpart of ferritin M subunit from rock bream (*Oplegnathus fasciatus*): an active constituent in iron chelation and DNA protection against oxidative damage, with a modulated expression upon pathogen stress. Fish Shellfish Immunol. 35, 1455–1465.
Graham, R.M., Chua, A.C., Herbison, C.E., Olynyk, J.K., Trinder, D., 2007. Liver iron transport. World J. Gastroenterol. 13, 4725–4736.
Hausmann, K., Wulfhekel, U., Düllmann, J., Kuse, R., 1976. Iron storage in macrophages and endothelial cells. Histochemistry, ultrastructure, and clinical significance. Blut 32, 289–295.
Iannello, A., Debbeche, O., Martin, E., Attalah, L.H., Samarani, S., Ahmad, A., 2005. Viral strategies for evading antiviral cellular immune responses of the host. J. Leukoc. Biol. 79, 16–35.
Kang, J.-H., 2010. Oxidative damage of DNA induced by ferritin and hydrogen peroxide. Bull. Korean Chem. Soc. 31, 2873–2876.
Keren, H., Lev-Maor, G., Ast, G., 2010. Alternative splicing and evolution: diversification, exon definition and function. Nat. Rev. Genet. 11, 345–355.
Knutson, M., Oukka, M., Koss, L.M., Aydemir, F., Wessling-Resnick, M., 2005. Iron release from macrophages after erythrophagocytosis is up-regulated by ferroportin 1 overexpression and down-regulated by hepcidin. Proc. Natl. Acad. Sci. U.S.A. 102, 1324–1328.
Krewulak, K.D., Vogel, H.J., 2008. Structural biology of bacterial iron uptake. Biochim. Biophys. Acta 1778, 1781–1804.
Lawson, D.M., Artymiuk, P.J., Yewdall, S.J., Smith, J.M., Livingstone, J.C., Treffry, A., Luzzago, A., Levi, S., Arosio, P., Cesareni, G., 1991. Solving the structure of human H ferritin by genetically engineering intermolecular crystal contacts. Nature 349, 541–544.
Lawson, D.M., Treffry, A., Artymiuk, P.J., Harrison, P.M., Yewdall, S.J., Luzzago, A., Cesareni, G., Levi, S., Arosio, P., 1989. Identification of the ferroxidase centre in ferritin. FEBS Lett. 254, 207–210.
Liu, H., Takano, T., Peatman, E., Abernathy, J., Wang, S., Sha, Z., Kucuktas, H., Xu, D.H., 2010. Molecular characterization and gene expression of the channel catfish ferritin H subunit after bacterial infection and iron treatment. J. Exp. Zool. A Ecol. Genet. Physiol. 313, 359–388.
Livak, K.J., Schmittgen, T.D., 2001. Analysis of relative gene expression data using real-time quantitative PCR and the 2(−Delta Delta C(T)) method. Methods 25, 402–408.

Luo, Y., Henle, E.S., Linn, S., 1996. Oxidative damage to DNA constituents by iron-mediated fenton reactions. The deoxycytidine family. J. Biol. Chem. 30, 21167–21176.
Missirlis, F., Holmberg, S., Georgieva, T., Dunkov, B.C., Rouault, T.A., Law, J.H., 2006. Characterization of mitochondrial ferritin in *Drosophila*. Proc. Natl. Acad. Sci. U.S.A. 103, 5893–5898.
Mohanty, B.R., Sahoo, P.K., 2007. Edwardsiellosis in fish: a brief review. J. Biosci. 32, 1331–1344.
Neves, J.V., Wilson, J.M., Rodrigues, P.N., 2009. Transferrin and ferritin response to bacterial infection: the role of the liver and brain in fish. Dev. Comp. Immunol. 33, 848–857.
Ong, S.T., Ho, J.Z., Ho, B., Ding, J.L., 2006. Iron-withholding strategy in innate immunity. Immunobiology 211, 295–314.
Outten, F.W., Theil, E.C., 2009. Iron-based redox switches in biology. Antioxid. Redox Signal. 11, 1029–1046.
Parmley, J.L., Urrutia, A.O., Potrzebowski, L., Kaessmann, H., Hurst, L.D., 2007. Splicing and the evolution of proteins in mammals. PLoS Biol. 5, 343–353.
Parthasarathy, N., Torti, S.V., Torti, F.M., 2002. Ferritin binds to light chain of human H-kininogen and inhibits kallikrein-mediated bradykinin release. Biochem. J. 365, 279–286.
Salinas-Clarot, K., Gutiérrez, A.P., Núñez-Acuña, G., Gallardo-Escárate, C., 2011. Molecular characterization and gene expression of ferritin in red abalone (*Haliotis rufescens*). Fish Shellfish Immunol. 30, 430–433.
Santambrogio, P., Levi, S., Cozzi, A., Corsi, B., Arosio, P., 1996. Evidence that the specificity of iron incorporation into homopolymers of human ferritin L- and H-chains is conferred by the nucleation and ferroxidase centres. Biochem. J. 314, 139–144.
Scudiero, R., Trinchella, F., Riggio, M., Parisi, E., 2007. Structure and expression of genes involved in transport and storage of iron in red-blooded and hemoglobin-less antarctic notothenioids. Gene 397, 1–11.
Seki, S., Habu, Y., Kawamura, T., Takeda, K., Dobashi, H., Ohkawa, T., Hiraide, H., 2000. The liver as a crucial organ in the first line of host defense: the roles of Kupffer cells, natural killer (NK) cells and NK1.1 $Ag^+$ T cells in T helper 1 immune responses. Immunol. Rev. 174, 35–46.
Skulachev, V.P., 1998. Possible role of reactive oxygen species in antiviral defense. Biochemistry 63, 1438–1440.
Theil, E.C., 1987. Ferritin: structure, gene regulation, and cellular function in animals, plants, and microorganisms. Annu. Rev. Biochem. 56, 289–315.
Theil, E.C., 2007. Coordinating responses to iron and oxygen stress with DNA and mRNA promoters: the ferritin story. Biometals 20, 513–521.
Thomson, A.M., Rogers, J.T., Leedman, P.J., 1999. Iron-regulatory proteins, iron-responsive elements and ferritin mRNA translation. Int. J. Biochem. Cell Biol. 31, 1139–1152.
Torti, F.M., Torti, S.V., 2002. Regulation of ferritin genes and protein. Blood 99, 3505–3516.
Tamura, K., Dudley, J., Nei, M., Kumar, S., 2007. MEGA4: Molecular Evolutionary Genetics Analysis (MEGA) software version 4.0. Mol. Biol. Evol. 24, 1596–1599.
Umasuthan, N., Whang, I., Kim, J.O., Oh, M.J., Jung, S.J., Choi, C.Y., Yeo, S.Y, Lee, J.H., Noh, J.K., Lee, J., 2011. Rock bream (*Oplegnathus fasciatus*) serpin, protease nexin-1: transcriptional analysis and characterization of its antiprotease and anticoagulant activities. Dev. Comp. Immunol. 35, 785–798.
Wang, W., Knovich, M.A., Coffman, L.G., Torti, F.M., Torti, S.V., 2010. Serum ferritin: past, present and future. Biochim. Biophys. Acta 1800, 760–769.
Watt, R.K., 2011. The many faces of the octahedral ferritin protein. Biometals 24, 489–500.
Whang, I., Lee, Y., Kim, H., Jung, S.J., Oh, M.J., Choi, C.Y., Lee, W.S., Kim, S.J., Lee, J., 2011a. Characterization and expression analysis of the myeloid differentiation factor 88 (MyD88) in rock bream *Oplegnathus fasciatus*. Mol. Biol. Rep. 38, 3911–3920.
Whang, I., Lee, Y., Lee, S., Oh, M.J., Jung, S.J., Choi, C.Y., Lee, W.S., Kim, H.S., Kim, S.J., Lee, J., 2011b. Characterization and expression analysis of a goose-type lysozyme from the rock bream *Oplegnathus fasciatus*, and antimicrobial activity of its recombinant protein. Fish Shellfish Immunol. 30, 532–542.
Wink, D.A., Hines, H.B., Cheng, R.Y., Switzer, C.H., Flores-Santana, W., Vitek, M.P., Ridnour, L.A., Colton, C.A., 2011. Nitric oxide and redox mechanisms in the immune response. J. Leukoc. Biol. 89, 873–891.
Worwood, M., 1990. Ferritin. Blood Rev. 4, 259–269.
Worwood, M., Brook, J.D., Cragg, S.J., Hellkuhl, B., Jones, B.M., Perera, P., Roberts, S.H., Shaw, D.J., 1985. Assignment of human ferritin genes to chromosomes 11 and 19q13.3-19qter. Hum. Genet. 69, 371–374.
Wu, C., Zhang, W., Mai, K., Xu, W., Wang, X., Ma, H., Liufu, Z., 2010. Transcriptional up-regulation of a novel ferritin homolog in abalone *Haliotis discus hannai* Ino by dietary iron. Comp. Biochem. Physiol. C Toxicol. Pharmacol. 152, 424–432.
Yamashita, M., Ojima, N., Sakamoto, T., 1996. Molecular cloning and cold-inducible gene expression of ferritin H subunit isoforms in rainbow trout cells. J. Biol. Chem. 271, 26908–26913.
Yang, T.C., Lai, C.C., Shiu, S.L., Chuang, P.H., Tzou, B.C., Lin, Y.Y., Tsai, F.J., Lin, C.W., 2010. Japanese encephalitis virus down-regulates thioredoxin and induces ROS-mediated ASK1-ERK/p38 MAPK activation in human promonocyte cells. Microbes Infect. 12, 643–651.
Zhang, X., Wei, W., Wu, H., Xu, H., Chang, K., Zhang, Y., 2010. Gene cloning and characterization of ferritin H and M subunits from large yellow croaker (*Pseudosciaena crocea*). Fish Shellfish Immunol. 28, 735–742.
Zheng, W.J., Hu, Y.H., Sun, L., 2010a. Identification and analysis of a *Scophthalmus maximus* ferritin that is regulated at transcription level by oxidative stress and bacterial infection. Comp. Biochem. Physiol. 156, 222–228.
Zheng, W.J., Hu, Y.H., Xiao, Z.Z., Sun, L., 2010b. Cloning and analysis of a ferritin subunit from turbot (*Scophthalmus maximus*). Fish Shellfish Immunol. 28, 829–836.
Zhou, J., Wang, W., Ma, G., Wang, A., He, W., Wang, P., 2008. Gene expression of ferritin in tissue of the Pacific white shrimp, *Litopenaeus vannamei* after exposure to pH stress. Aquaculture 275, 356–360.